arXiv:2609.35220v1 [math.OC] 28 Sep 2026

Robust identification of drive-by sensing ride-hailing market with Points of Interest monitoring under uncertain ride demand

Binzhou Yang [a,b*] Bin Shuai [a,b] Minhao Xu [c] Boyang Du [d]

a Institute of System Science and Engineering, Southwest Jiaotong University, China
b School of Transportation and Logistics, Southwest Jiaotong University, China
c School of Automation and Electrical Engineering, Lanzhou Jiaotong University, China
d School of Economics and Management, Southwest Jiaotong University, China

September 29, 2026

Abstract

Taxi-based mobile sensing has emerged as a cost-efficient paradigm for large-scale urban environmental monitoring. In practice, both passive and active sensing strategies are adopted by ride-hailing platforms. Passive sensing, conducted during passenger-serving trips, is constrained by stochastic and spatially imbalanced ride demand, leading to limited and uneven coverage. Active sensing, executed by vacant taxis, provides greater control over sensing operations but incurs additional operational costs, and is thus typically treated as a supplementary strategy. To address the inefficiencies of the conventional "passive-first, active-second" paradigm, which may delay the monitoring of critical Points of Interest (POIs) and increase system-wide costs, we propose a Distributionally Robust Optimization (DRO)-based framework for active mobile sensing. First, we develop an enhanced A*-based drive-by sensing routing policy that integrates vehicle-task matching while capturing both global routing efficiency and local sensing opportunities. Second, we formulate the active sensing problem as a DRO model that explicitly accounts for uncertainty in ride demand through an ambiguity set of probability distributions, enabling robust decision-making for vacant taxi routing and vehicle-task matching. The proposed framework is evaluated on both static and dynamic mobile sensing settings using real-world data. Computational results demonstrate that our approach achieves better performance in terms of sensing coverage, operational cost, and robustness compared to benchmark strategies, highlighting the value of integrating distributional robustness into taxi-based sensing operations.

Keywords: Drive-by sensing; Ride-hailing service; Enhanced A drive-by sensing route; Distributionally robust optimization*

1 Introduction

By integrating Drive-by Sensing (DS) into urban transport vehicles, various sensing scenarios can be realized by leveraging the hosts' high mobility and low maintenance costs. These scenarios include air quality monitoring, traffic state estimation, noise monitoring, urban heat

*Corresponding author, e-mail: ybz@my.swjtu.edu.cn ;

island effect analysis, parking availability detection, and built environment assessment (Mathur et al., 2010; Pasqualetti et al., 2012; Gao et al., 2016; Bock et al., 2017; Ali and Dyo, 2017; Cruz et al., 2020a,b; Tonekaboni et al., 2020; Xu et al., 2020; Song et al., 2021; Yu et al., 2021; Guo et al., 2022). Meanwhile, following a decade of rapid growth, the ride-hailing industry has seen a marked slowdown in the U.S. and China, its two largest markets, with fierce competition driving platforms to explore new value-added services beyond passenger transportation, such as providing food or freight delivery service, engaging with the third-party integrators (Wu et al., 2020; Liu et al., 2025). In this context of DS, ride-hailing vehicles offer distinct advantages over fixed or dedicated sensing fleets, including dense urban coverage, long operating hours, and the potential for coordinated sensing task allocation.

Due to platform dispatch protocols, monitoring is primarily limited to analyzing the spatio-temporal distribution of completed trips and the cruising of vacant taxis. While existing literature has explored sensor deployment, operational interventions, and incentive mechanisms for vehicle-based sensing (Zhao et al., 2015; Bonola et al., 2016; Bock et al., 2017; Martino and Lucio Starace, 2022; Yang et al., 2025), the majority of these works assume static or dedicated fleets and neglect the dynamic, demand-driven trajectories of ride-hailing vehicles. The resulting blind spots undermine the completeness of urban coverage data, introducing uncertainty and risk into subsequent urban management and governance (Bock et al., 2017; O'Keeffe et al., 2019; Asprone et al., 2021; Liu et al., 2025). In contrast to prior work on sensing coverage for road area sources (1 km $\times$ 1 km grids in road networks), this study focuses on sensing coverage for point sources at monitoring blind spots furthermore, that is, Points of Interest (POIs) for road network monitoring. Thus, a fundamental challenge in existing research is the tension between leveraging opportunistic vehicle mobility for road segment monitoring and meeting the targeted spatio-temporal monitoring tasks, see Section 2.1 for further details. Indeed, on a ride-hailing platform with DS capabilities, aggregate POIs monitoring demand is often evaluated at a strategic level. Such an assessment, however, inherently overlooks the dynamics, uncertain conditions of real-time ride demand, which influences the POI monitoring.

To accomplish the sensing tasks throughout the monitoring time domain, the prevailing design of the DS ride-hailing market, which focuses on maximizing sensing gain via continuous order dispatch (Yang et al., 2025), must be supplanted by a framework that incorporates uncertainties inherent to ride-hailing operational characteristics, see Section 2.2 for details. The realization of such a framework faces critical issues: (1) accurate matching and routing planning for occupied taxis, as generated by the platform's operational objectives for a mixed DS fleets; and (2) task assignment and monitoring routes for vacant instrumented taxis. To address the above two key issues, the vehicle-passenger and vehicle-task matching schemes developed in this paper establish that its monitoring metric adopts priority-based matching (Iwase et al., 2026; Wang et al., 2026; Kwon et al., 2026). The purpose of the former is to use passive sensing to maximize sensing utility while maintaining service levels (e.g., customer wait time and matching rate) for regular riders by prioritizing trip requests. On this basis, the latter aims to complete as many POI monitoring tasks as possible through active sensing, while achieving high sensing efficiency in road monitoring coverage over a short period. Under active sensing, the vacant instrumented taxis are controllable, the platform performs task assignment and route planning, and incurs the corresponding operation costs to incentivize POI monitoring. This paper subsequently proposes a robust framework account for vacant instrumented taxi routing and vehicle-task matching, which explicitly characterizes the associated uncertainties and POI monitoring cost. The technical approach of the proposed framework is summarized as follows.

Guided by the "passive-first, active-second" paradigm, in each decision-making epoch, trip

requests are distributed to instrumented taxis first to maximize sensing utility, and then to non-instrumented taxis to meet ride demand. To supplement the above passive sensing, an A*-based drive-by sensing routing policy is implemented through active POI-monitoring. The matching and routing pairs of vacant instrumented taxis and tasks are constructed to characterize the interplay between local sensing opportunities and global routing efficiency. In detail, integrating the dual spatial scales of grid-level coverage and network-level routing, as many monitoring tasks as possible are assigned to vacant instrumented taxis in a time-efficient manner that maximizes local sensing utility. The final generated vehicle–task matching and routing pairs guarantee global efficiency. Subsequently, to address the uncertainties inherent in the DS ride-hailing platform's monitoring operations (e.g., daily travel demand fluctuations), a Distributionally Robust Optimization (DRO) model is employed and adapted to manage the monitoring costs associated with the designed routes for vacant instrumented taxis. Finally, a data-driven approach is employed to calibrate the uncertainty set within the DRO framework, enabling it to applicable for different operational control resolutions.

The main contributions of this study are as follows:

Conception and model: This work proposes a feasible enhanced A*-based drive-by sensing route service policy to determine the matches between vacant instrumented taxis and POI monitoring tasks, thereby ensuring local opportunistic sensing and global routing efficiency. Simulations confirm that the generated matching and routing pairs can complement the data collection blind spots while achieving high timeliness in road sensing coverage.

Theoretical properties: This paper presents the first application of the DRO technique within the DS ride-hailing market. The DRO technique provides an approach for optimizing the operation cost incurred by POI monitoring with robust outcomes. It captures the interactive effects of the platform's uncertain ride demand on POI monitoring, without requiring assumptions about the individual or joint distributions of these uncertain variables.

Practical significance: The proposed data-driven uncertainty set calibration is highly practical for the mixed-fleet DS ride-hailing market, enabling the DRO model to operate at different control resolutions (e.g., predetermined and adaptive). Furthermore, the calibration method can be readily generalized to account for varying data availability under day-to-day, within-day, and seasonal conditions.

The remainder of this paper is structured as follows. Section 2 reviews the relevant literature. Section 3 details the proposed methodology, a simulation-based case study is presented in Section 4. Finally, Section 5 discusses the framework's potential for enhancing the operational performance of a DS ride-hailing market with a mixed fleets, and Section 6 provides concluding remarks.

2 Related work

In this section, we provide a research survey of sensing operations for taxi fleets (Section 2.1), POI monitoring with uncertain ride demand (Section 2.2) and robust optimization approaches in transportation service (Section 2.3). Notably, under the uncertainty of POI sensing, our study addresses a research gap in the DS ride-hailing market with the aim of optimizing monitoring cost expenditures.

2.1 Sensing operations for taxi fleets

Data collected from instrumented vehicles, with minimal interference to fleet operations, exemplifies the opportunistic sensing capabilities of taxi fleets. Utilizing empirical taxi data

from Rome, Bonola et al. (2016) demonstrated that a fleet of 120 vehicles could achieve 80% coverage of the downtown area within 24 hours. Highlighting the suitability of taxi fleets for scouting on-street parking availability, Bock et al. (2017) found that approximately 500 taxis could adequately cover 90% of road segments in San Francisco, despite the spatio-temporal heterogeneous distribution of movement patterns. O'Keeffe et al. (2019) analyzed the sensing capability of taxi fleets in several major cities using a ball-in-bin model, verifying considerably limited sensing capabilities due to the heterogeneous distribution of taxi trajectories. Regarding the optimal subset selection of drive-by sensing taxi fleets, Chen et al. (2017) proposed a greedy heuristic to select trajectory segments that maximize sensing quality under limited costs. In their postulated scenario, the sensing cost was proportional to the trajectory length when the sensor was manually activated. Zhang et al. (2018) jointly optimized total coverage across all vehicles and the reliability of individual sensing tasks, modeling the problem as a bi-objective optimization to determine vehicle selection. Taking into account host vehicle speeds and their impact on sensing quality, Yu et al. (2021) proposed a vehicle selection model for traffic condition monitoring based on the spatio-temporal characteristics of the road network.

Operational interventions and incentives have been proposed to enhance the sensing coverage performance of taxi fleets. A primary focus is on routing interventions for given origin-destination pairs. For instance, Masutani (2015) seeks to maximize sensing quality by providing routing recommendations to vehicles. Asprone et al. (2021) proposed an ε-perturbed route set, generated by deviating from the shortest path (computed via the A-star algorithm), to optimize the spatial coverage of a taxi fleet. Similarly, Guo and Qian (2024) provided routing guidance to vacant taxis during their cruising phase. Liu et al. (2025) classified taxi types and utilized instrumented taxis for monitoring targeted objectives via the shortest path; however, their methodology fails to capture the utility of road segment sensing coverage. Regarding incentive schemes, Fan et al. (2021) designed a joint scheduling and pricing model to reward drivers for taking routes within an acceptable detour range, thereby encouraging coverage of broader areas. Xu et al. (2020) formulated both routing advice and monetary incentives to maximize the sensing gain of vacant taxis cruising for their next customer. These incentive-based strategies were optimized using an efficient algorithm named iLOCuS. Furthermore, Chen et al. (2020) addressed the problem by matching riders with vacant taxis while providing routing suggestions, aiming to maximize sensing coverage under a limited incentive budget. This framework was integrated with a prediction-based actuation system called PAS.

Previous research has primarily focused on enhancing the overall sensing capabilities of taxi fleets, often overlooking specific target sensing objects. Consequently, the collected spatio-temporal data may lack statistical significance for targeted monitoring tasks. To address the demand for POI monitoring, this study leverages vacant instrumented taxis, which exhibit high controllability and flexibility. These vehicles are tasked to either complement the sensing capabilities of other fleets or to perform highly-targeted sensing missions. This objective is achieved by continuously coordinating sensing demand with travel demand through the implementation of an enhanced A* drive-by sensing route policy.

2.2 POI monitoring with uncertain ride demand

Instrumented taxis collect data on the urban physical environment by scanning road segments, whether engaged in customer transport or in vacant cruising. The collected data serves as an input for governmental urban management.

Existing researches have focused on two main approaches to accomplish monitoring tasks: utilizing the inherent mobility of vehicles during transportation services, or executing pre-

defined monitoring assignments. On leveraging the inherent mobility of vehicles, Despite demonstrating the suitability of taxi fleets for large-scale urban sensing (e.g., on-street parking availability as in Bock et al. (2017)), research also underscores a critical flaw: reliance on opportunistic, mobility-driven data collection leads to incomplete road coverage and spatio-temporal biases, which in turn create substantial uncertainty in the monitoring data. Bock et al. (2017) found that approximately 500 taxis could cover 90% of road segments in San Francisco, yet this coverage remains inherently uneven due to heterogeneous movement patterns. Complementing this, O'Keeffe et al. (2019) used a ball-in-bin model to verify that the sensing capability of taxi fleets in several major cities is considerably limited precisely because of the uneven distribution of taxi trajectories. Together, these studies indicate that the very mobility which enables sensing also guarantees gaps in coverage, generating uncertainty that must be explicitly addressed. Regarding the predefined monitoring tasks, Asprone et al. (2021) compare the spatio-temporal coverage of probe vehicles routed by the A^* algorithm against that achievable under the RA^*_ε algorithm, across varying ε values. This comparison is conducted on datasets of real-world taxi trajectories, considering specified source (s) and target (t) points. Liu et al. (2025) present the distribution pattern of monitoring POIs within the Manhattan network and employs a transportation-service-compatible shortest route planning strategy for vacant instrumented taxis.

From the strategic level of the DS ride-hailing platform. A key limitation of prior work is its failure to account for the POI monitoring with uncertain ride demand when utilizing instrumented taxis for road segment sensing. This problem results in inherent gaps in coverage and persistent data blind spots. Consequently, the effectiveness of subsequent monitoring-data-based urban governance is compromised. To address this issue, this paper formulates and solves a priority-based matching and routing problem that jointly considers road segment sensing, ride-hailing services and POI monitoring demand with uncertainty.

2.3 Robust optimization approaches in transportation

Robust optimization is a methodology that addresses uncertainty by seeking solutions that remain feasible under the worst-case realization within a predefined uncertainty set. Since the publication of several seminal works in the late 1990s, robust optimization has seen substantial developments in both its theoretical foundations and practical applications. Compared to stochastic programming, robust optimization mitigates the computational intractability that can arise from the high dimensionality of uncertain parameters. A key advantage of robust optimization is that it relaxes the stochastic programming assumption that precise probability distributions of uncertainties are known, an assumption that often does not hold in practice. Furthermore, as decision-makers are often risk-averse rather than risk-neutral, the conservative nature of robust optimization makes it particularly applicable.

DRO, first proposed by Scarf (1957) in the context of a newsvendor problem, integrates concepts from both robust and stochastic optimization. The DRO framework optimizes the worst-case expected value of the objective function over an ambiguity set of probability distributions, which is characterized by certain known parameters of the uncertainty. A significant body of research is devoted to the construction of different ambiguity sets. A common approach involves defining the ambiguity set using fixed-moment information, such as the mean and variance. A comprehensive survey of this area is provided by Goh and Sim (2010). Other methodologies include the work of Chen et al. (2007), who incorporated directional deviations to refine the description of the distribution set, and Delage and Ye (2010), who investigated a general DRO framework where the mean and covariance of the underlying uncertainties are

subject to uncertainty. Both robust and distributionally robust optimization are widely applied in transportation, including route choice (Qi et al., 2016), user equilibrium (Ahipasaoglu et al., 2015), network design (Ng and Lo, 2016), air traffic flow pattern identification (Sidiropoulos et al., 2017), routing optimization (Jaillete et al., 2016; Zhang et al., 2021), facility location (Ardestani-Jaafari and Delage, 2017), and network sensor location (Zhu et al., 2018).

Existing research indicates that DRO techniques are capable of evaluating additional expenditures, such as monitoring costs, within a robust framework. However, a research gap remains in evaluating the extra operational cost associated with monitoring POIs using vacant instrumented taxis. To bridge this gap, this paper constructs an uncertainty set for the extra monitoring cost under a designated monitoring pattern. By leveraging DRO techniques, we aim to minimize the expected cost expenditure under the worst-case scenario, thereby effectively capturing the potential uncertainties associated with the mixed DS ride-hailing platform operation under uncertain ride demand. Furthermore, this work provides an extensible framework for the ride-hailing market, with potential contributions to the strategic management of monitoring costs.

3 Method

This section describes several elements that are essential to the main discussion of the robust identification method under uncertain ride demand, namely the background materials of DS ride-hailing market operation with POIs monitoring in Section 3.1, which includes the quantification of sensing externality in Section 3.1.1, a priority-based matching process in the context of DS in Section 3.1.2 and the drive-dy sensing coverage problem with POI monitoring in Section 3.1.3, the enhanced A* drive-by sensing route service policy for POIs monitoring in Section 3.2, DRO extension of the deterministic formulation in Section 3.3.

Table 1 lists the notations to be used in the remainder of the paper.

Table 1: Mathematical symbols

Sets and indices	
$\mathcal{D}$	Set of drivers, indexed by $d \in \mathcal{D}$
$\mathcal{R}$	Set of riders, indexed by $r \in \mathcal{R}$
$\mathcal{D}^*$	Set of matched drivers
$\mathcal{R}^*$	Set of matched riders
T	Set of sensing intervals $t \in T$
$\mathcal{N}$	Set of nodes
$\mathcal{G}$	Set of grids
$\mathfrak{R}_G$	Set of G-route
$\mathfrak{R}_N$	Set of N-route
Parameters and constants	
$l = (d, r)$	A potential match of driver d and rider r
Γ	The overall sensing utility
Θ	Sensing utility
ϑ_{dr}	Sensing externality of a matched trip $l = (d, r)$
τ_{dr}	Pick-up distance from the current location of driver d to rider r
w_{dr}	The customer wait time of a matched trip $l = (d, r)$
N_1	Instrumented taxi fleets size

Continued on next page

Table 1 (continued): Mathematical symbols

Sets and indices	
N_0	Non-instrumented taxi fleets size
Decision variables	
x_{dr}	Equals 1 if driver d and rider r are matched, and 0 otherwise

3.1 Background of DS ride-hailing market operation with POIs monitoring

3.1.1 Quantifying drive-by sensing (DS) externality

For a discretized spatio-temporal sensing framework, let G denote the set of unit grid cells (each $1\,\text{km} \times 1\,\text{km}$) partitioning the target region, and let T index discrete sensing intervals (e.g., hourly). The overall sensing utility is:

$$\Gamma = \sum_{t \in T} \mu_t \sum_{g \in G} s_g \, \Theta_{g,t}(\Lambda_{g,t}), \tag{3.1}$$

with normalized temporal weights μ_t ($\sum_{t \in T} \mu_t = 1$) and spatial weights s_g ($\sum_{g \in G} s_g = 1$) reflecting sensing priorities. For grid $g \in G$ during interval $t \in T$, the sensing utility is defined as:

$$\Theta_{g,t}(\Lambda_{g,t}) = (\Lambda_{g,t})^{\rho}, \quad \rho \in (0, 1), \tag{3.2}$$

where $N_{g,t}$ is the number of distinct vehicles visiting grid g in interval t. The exponent ρ captures diminishing marginal returns, discouraging overconcentration of visits. We set $\rho = 0.2$ for our air-quality monitoring case study (Ji et al., 2023; Han et al., 2024).

In online driver-rider matching, each sensing interval t is subdivided into decision epochs s_i ($i = 1, \ldots, n$). For a candidate match $l = (d, r)$ considered at epoch s_i, its marginal utility is:

$$\vartheta_{dr} = \sum_{t \in T} \mu_t \sum_{g \in G_{dr}} s_g \left((\Lambda_{g,t,s_i} + 1)^{\rho} - (\Lambda_{g,t,s_i})^{\rho} \right), \tag{3.3}$$

where $G_{dr} \subset G$ is the set of grids traversed by trip l, and Λ_{g,t,s_i} is the cumulative vehicle count for grid g in interval t as of epoch s_i.

3.1.2 A priority-based matching process in the context of DS

Taxis are divided into instrumented (fixed size N_1) and non-instrumented (fixed size N_0) fleets. In the context of DS, the matching process is priority-based to serve the platform's operations (Iwase et al., 2026; Wang et al., 2026; Kwon et al., 2026). As illustrated in Figure 1, orders are first assigned to instrumented taxis to maximize sensing gain, then to non-instrumented taxis to optimize operational metrics with the objective of minimizing customer wait time. Any remaining vacant instrumented taxis are dispatched to monitoring POIs to fulfill sensing tasks.

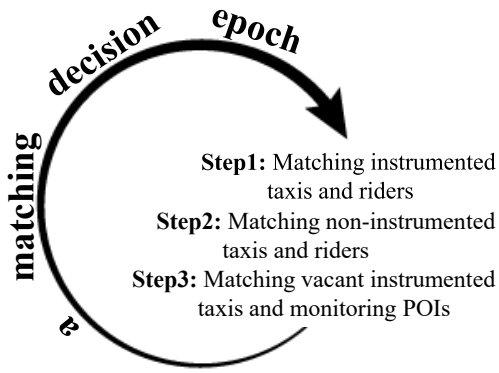

Figure 1: Matching process in a decision epoch

In Step 1, the objective focuses on the sensing gain ϑ_{dr} for a matched trip, which is calculated using Eq. (3.3). This calculation assumes that the route is known in advance and follows the shortest path. The matching model aims to maximize the total sensing externality, formulated as:

$$\text{[Sensing utility]} \quad \max_{x=(x_{dr})_{d\in\mathcal{D},r\in\mathcal{R}}} U = \sum_{r\in\mathcal{R}}\sum_{d\in\mathcal{D}} \vartheta_{dr} x_{dr} \tag{3.4}$$

$$\text{s.t.} \sum_{r\in\mathcal{R}} x_{dr} \leq 1, \quad \forall d \in \mathcal{D} \tag{3.5}$$

$$\sum_{d\in\mathcal{D}} x_{dr} \leq 1, \quad \forall r \in \mathcal{R} \tag{3.6}$$

$$x_{dr} \in \{0,1\}, \quad \forall d \in \mathcal{D},\, r \in \mathcal{R} \tag{3.7}$$

Here, the binary decision variable x_{dr} equals 1 if driver d and rider r are matched.

In Step 2, the objective shifts to minimizing the customer wait time w_{dr} for a matched trip $l = (d, r)$, assuming travel along the shortest route. Consequently, the matching model for this step is formulated as follows:

$$\text{[Customer wait time]} \quad \min_{x=(x_{dr})_{d\in\mathcal{D},r\in\mathcal{R}}} W = \sum_{r\in\mathcal{R}}\sum_{d\in\mathcal{D}} w_{dr} x_{dr} \tag{3.8}$$

$$\text{s.t.} \sum_{r\in\mathcal{R}} x_{dr} \leq 1, \quad \forall d \in \mathcal{D} \tag{3.9}$$

$$\sum_{d\in\mathcal{D}} x_{dr} \leq 1, \quad \forall r \in \mathcal{R} \tag{3.10}$$

$$x_{dr} \in \{0,1\}, \quad \forall d \in \mathcal{D},\, r \in \mathcal{R} \tag{3.11}$$

The binary decision variable x_{dr} equals 1 if driver d and rider r are matched. The continuous variable w_{dr} denotes the resulting customer wait time for this match.

In Step 3, the matching process involves vacant instrumented taxis and monitoring POIs, with the specific objectives and routing strategies detailed in Section 3.1.3.

3.1.3 The drive-by sensing coverage problem with POI monitoring

The Drive-by Sensing Coverage (DSC) problem is proposed by Han et al. (2024) firstly. Unlike classical facility location with fixed sensors, DSC employs instrumented taxis as mobile sensors, extending the traditional framework (Riahi et al., 2021; Wang et al., 2021; Viti et al., 2014). The problem of routing instrumented taxis for data collection has two key aspects: (i) sensing utility is accrued via grid intersections rather than node/arc visits, and (ii) utility follows a diminishing-returns function $\Theta_{g,t}(\cdot)$. The primary challenge in coordinating grid-level coverage with network-level routing lies in their coupling across disparate spatial resolution scales.

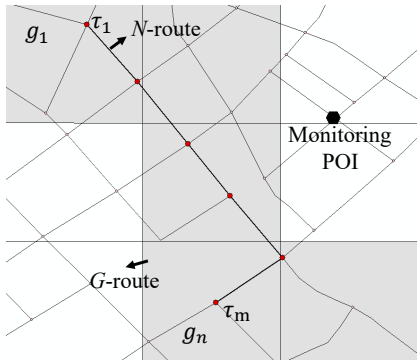

Figure 2: Drive-by sensing coverage with POI monitoring. Adapted from "Exploring the sensing power of mixed vehicle fleets" by Han et al. (2024), Transportation Research Part B: Methodological. 190, 103066 (https://doi.org/10.1016/j.trb.2024.103066). Copyright 2024 by Elsevier.

In this paper, considering monitoring blind spot coverage to supplement monitoring data, we extend the DSC monitoring problem to the DSC problem with POI monitoring. As illustrated in Figure 2, a N-route (where N stands for network) refers to a conventional route represented as a sequence of nodes $\kappa_N = (\tau_1, \ldots, \tau_m) \subset \mathcal{N}$. A G-route (where G stands for grid) refers to a conceptual route expressed as the sequence of grids traversed, $\kappa_G = (g_1, \ldots, g_n) \subset \mathcal{G}$ (Han et al., 2024). A node $\tau \in \mathcal{N}$ is said to belong to a grid $g \in \mathcal{G}$ (denoted $\tau \in g$) if it lies within that grid, and Figure 2 shows a POI to be monitored through a marked node. Therefore, accurately characterizing the spatio-temporal patterns of POI monitoring demand is essential for effectively utilizing the available fleet of vacant instrumented taxis. The design of efficient matching and routing algorithms for POI monitoring at dual spatial scales is detailed in Section 3.2.

Remark 3.1. *Building on the deterministic formulation presented in Section 3.2, which assumes prior and accurate knowledge of POI monitoring demand, we provide the monitoring path policy for POIs. From an operational perspective, the generated monitoring path of vacant instrumented taxis for POIs directly determines the POI monitoring cost (i.e. operating cost of vacant instrumented taxis for POI monitoring). Nevertheless, the resulting solutions of monitoring cost may lack robustness against potential variations in demand distribution caused by multiple sources of uncertainty.*

To overcome this limitation, we adopt a data-driven distributionally robust optimization (DRO) approach. The detailed formulation is provided in Section 3.3. DRO addresses uncertainty in both parameters and their underlying distributions, which are difficult to estimate accurately from limited or interdependent data. Unlike conventional robust optimization, it

avoids excessive conservatism by optimizing against the worst-case distribution within a plausibly specified family. We propose a data-driven ϕ-divergence-based calibration method to construct the uncertainty set. Leveraging empirical statistics and risk preferences with sufficient data, the proposed test defines distributions that are close to the empirical estimate.

3.2 Enhanced A* drive-by sensing route service policy for POI monitoring

3.2.1 POI monitoring routing for a vacant instrumented taxi

For a single instrumented taxi, we consider a matching and routing problem defined from an origin node τ in the road network. The overall objective is to determine a destination node τ_m (which represents a monitoring POI) along with the corresponding N-route and G-route to the target grid, so as to gather sensing utilities in a time-efficient manner. Given the origin node $\tau_1 \in g_1 \in \mathcal{G}$ in the road network and taking into account Eq. (3.3), the problem amounts to identifying vehicle-task matching pairs with the utility time-efficiency function $\varphi(\cdot)$.

$$\varphi(d\tau) = \frac{\vartheta_{\bar{\kappa}(\tau_1;\kappa_G)}}{T_{\bar{\kappa}(\tau_1;\kappa_G)}} \tag{3.12}$$

where the N-route fully implements the G-route $\kappa_G = (g_1, \ldots, g_n) \in \mathfrak{R}_G$ with starting node $\tau_1 \in g_1$, which is denoted $\bar{\kappa}(\tau_1; \kappa_G) \in \mathfrak{R}_N$. In each matching decision epoch, monitoring POIs are assigned to instrumented taxis through the following matching model.

$$\max_{x=(x_{d\tau})_{d\in\mathcal{D},\tau\in\mathcal{N}}} Q = \sum_{\tau\in\mathcal{N}} \sum_{d\in\mathcal{D}} \varphi(d\tau) x_{d\tau} \tag{3.13}$$

$$\text{s.t.} \sum_{\tau\in\mathcal{N}} x_{d\tau} \leq 1, \ \forall d \in \mathcal{D} \tag{3.14}$$

$$\sum_{d\in\mathcal{D}} x_{d\tau} \leq 1, \ \forall \tau \in \mathcal{N} \tag{3.15}$$

$$x_{d\tau} \in \{0, 1\}, \ \forall d \in \mathcal{D}, \tau \in \mathcal{N} \tag{3.16}$$

Here, the binary decision variable $x_{d\tau}$ indicates whether driver d is matched with monitoring POI τ, with the corresponding N-route $\bar{\kappa}(\tau_1; \kappa_G)$ generated by a modified A* algorithm. The utility time-efficiency $\varphi(d\tau)$ is defined as the ratio of the weighted marginal sensing utilities accumulated along the traversed G-route $G_{\bar{\kappa}(\tau_1;\kappa_G)}$ to the total travel time $T_{\bar{\kappa}(\tau_1;\kappa_G)}$. Maximizing $\varphi(d\tau)$ incentivizes taxis to prioritize grids with high marginal sensing utility, thereby accumulating greater utility within a shorter time window. In other words, the proposed algorithm is designed to incentivize vacant instrumented taxis to complete POI monitoring by preferentially traversing grids with high marginal sensing utility. This procedure is formally summarized in Table B.1.

3.2.2 POI monitoring routing for multiple vacant instrumented taxis

To account for overlapping search areas, we adopt a sequential optimization procedure that iteratively updates the marginal utilities of traversed grids until convergence or a maximum iteration limit is reached. Routes are planned within each discrete time window using the window-specific total sensing utility Γ, thereby avoiding redundant cross-window coverage and reducing the computational burden of long-horizon planning.

Algorithm 2's routing plan in Table B.2 is extended over the full time horizon T by converting the routes $R_1^D, \ldots, R_{n^D}^D$ into repeatable round trips, with each one-way leg executed

within a discrete time window t. Unlike conventional vehicle routing problems that assume fixed depots, instrumented taxi routes may originate from any road network node, provided that monitoring POI demand is satisfied (see Section 4.5 for an example).

3.3 DRO extension of the deterministic formulation

3.3.1 Introduction to the general data-driven DRO framework

Let $\mathbf{Q} = (\mathbf{Q}_t : t \in T)$ denote a random vector that affects the POI monitoring during each discrete sensing interval $t \in T$. In a more general context, $\mathbf{Q}$ can represent any uncertain variables or vectors related to ride demand uncertainty, either as exogenous inputs (e.g. city size, weather and population density) or endogenous variables (e.g. trip fare, fleet availability).

For each vacant instrumented taxi, the generated POI monitoring route (detailed in Section 3.2) is used to compute the POI monitoring cost, based on a unit-distance compensation of 1.5 CNY/km provided to the driver. The total monitoring cost borne by the mixed DS ride-hailing platform is the sum of the monitoring costs associated with all vacant instrumented taxis. Given a fixed variable x, which denotes the fleet size of instrumented taxis (N_1) in this study, the monitoring cost is considered as the objective function or Key Performance Indicator (KPI), denoted $KPI(x, \mathbf{Q})$, which is to be minimized and treated as a random variable parameterized by x.

$$KPI(x, \mathbf{Q}) = 1.5 \times \sum_{i=1}^{N_1} L_i(\mathbf{Q}) \tag{3.17}$$

where $x = N_1$ and $L_i(\mathbf{Q})$ denotes the per-unit-time POI monitoring route length (km) for instrumented taxi i.

This randomness arises from the stochasticity of $\mathbf{Q}$, and is assumed to follow an unknown probability distribution $D^*(x)$. In the absence of exact knowledge of $D^*(x)$, we instead consider an uncertainty set $\mho(x)$ comprising candidate probability distributions that are consistent with the available data via the ϕ-divergence test. Hence, given that the KPI (i.e., the objective function) is to be minimized, the DRO formulation is presented as follows:

$$\min_{x} \max_{D \in \mho(x)} E_D[KPI(x, \mathbf{Q})] \tag{3.18}$$

where E_D denotes the expectation KPI under the candidate probability distribution $D(x)$. The DRO model is formulated as a min-max optimization problem, which is non-convex and infinite-dimensional.

To ensure the practical solvability of the problem, we adopt a metaheuristic solution approach supported by a finite approximation of the PDF. Specifically, for the outer minimization problem in Eq. (3.18), metaheuristic search algorithms, such as the genetic algorithm (GA) and particle swarm optimization (PSO), can be employed to search for the optimal solution x^*, relying solely on the objective function values (i.e., the results of the inner maximization problem). Thus, it suffices to determine the solution to the inner maximization problem for any given x. The detailed implementation procedure is presented as follows.

We consider a set of M historical samples of the random vector $\mathbf{Q}$, denoted $(\mathbf{Q}^1, \mathbf{Q}^2, ..., \mathbf{Q}^M)$. Given the instrumented taxi fleet size x, the monitoring cost (i.e., the KPI) is computed based on the unit-distance compensation rule for vacant instrumented drivers (1.5 CNY/km). This computation is performed via simulation or a deterministic procedure, specifically the enhanced A^* drive-by sensing route service policy proposed in this study. Consequently, a sequence of

KPI samples is obtained, denoted as $KPI(x, \mathbf{Q}^1), KPI(x, \mathbf{Q}^2), ..., KPI(x, \mathbf{Q}^M)$, where each sample represents the monitoring cost derived from the k-th historical data sample $\mathbf{Q}^k$ (with $k = 1, 2, ..., M$). This sequence is defined as:

$$f^k = KPI(x, \mathbf{Q}^k), \quad 1 \leq k \leq M \tag{3.19}$$

where each f^k corresponds to a realization of the random variable $KPI(x, \mathbf{Q}^k)$. Without loss of generality, we assume these KPI samples are sorted in non-decreasing order, i.e., $f^1 \leq f^2 \leq ... \leq f^M$.

Definition 3.2. *ϕ-divergence is a distance measure between two vectors $\boldsymbol{p} = (p_1, p_2, ..., p_m) \geq 0$ and $\boldsymbol{q} = (q_1, q_2, ..., q_m) \geq 0$ in $\boldsymbol{R}^m$ and can be defined as:*

$$I_\phi(p, q) = \sum_{j=1}^{m} q_j \phi(\frac{p_j}{q_j}) \tag{3.20}$$

If p and q are probability vectors, there exists constraints $\sum_{j=1}^{m} p_j = 1$ and $\sum_{j=1}^{m} q_j = 1$. $\phi(u)$ is a convex function for $u > 0$.

Intuitively, ϕ-divergence is a mathematical measure used to quantify the discrepancy between two PDFs. To facilitate understanding, two discrete probability distributions are illustrated in Figure 3. For a given scenario j in Eq. (3.20), there exists a discrepancy between the probabilities associated with the two distributions, denoted p_j and q_j, respectively. The magnitude of this discrepancy is defined as $q_j \phi(\frac{p_j}{q_j})$, and the ϕ-divergence between the probability vectors $\mathbf{p}$ and $\mathbf{q}$ is defined as the sum of these terms over all scenarios $j = 1, 2, 3, ..., m$, i.e. $\sum_{j=1}^{m} q_j \phi(\frac{p_j}{q_j})$.

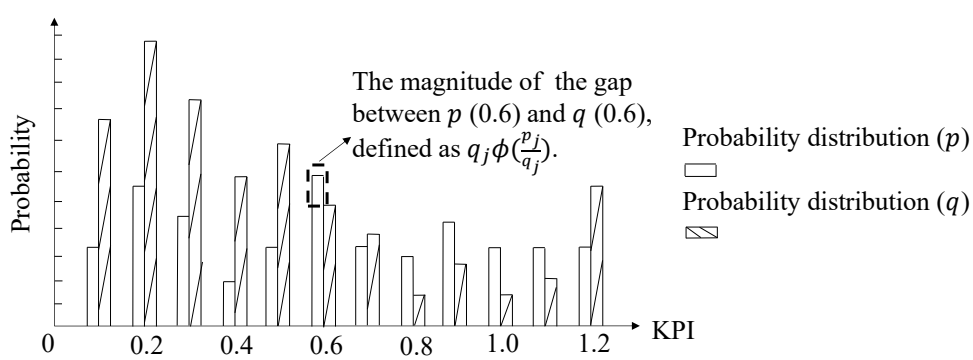

Figure 3: An illustration of phi-divergence.

Adopting a discrete probability framework, in contrast to a continuous one, reduces model complexity while retaining essential probabilistic characteristics. The corresponding uncertainty set is constructed as follows:

$$\mho(x) = \left\{ p_j = (p_1, p_2, ..., p_m) | I_\phi(p, q) \leq \rho, \sum_{j=1}^{m} p_j = 1, p_j \geq 0 \right\} \tag{3.21}$$

where ρ is a predefined parameter representing the uncertainty level. The formulation of $\mho(x)$ can accommodate various ϕ-divergence functions, allowing flexibility to align with decision-maker preferences. A comprehensive summary of these functions is provided in Table A.1.

The ϕ-divergence is grounded in the following hypothesis testing framework:

$$H_0 : D(x) = D^*(x), \quad H_A : D(x) \neq D^*(x) \tag{3.22}$$

where $D^*(x)$ is the unknown true distribution, and $D(x)$ is any nominal distribution. The null hypothesis H_0 is rejected at significance level α if the following holds (Ben-Tal et al., 2013):

$$T_\phi^M(p, q) = \frac{2M}{\phi''(1)} I_\phi(p, q) \tag{3.23}$$

where $T_\phi^M(p, q) \sim \chi^2_{m-1}$. The rejection of the null hypothesis H_0 is jointly determined by the sample data and a prescribed quantile of a specific distribution. For a comprehensive derivation, see Ben-Tal et al. (2013). The rejection rule is

$$T_\phi^M(p, q) > \chi^2_{m-1,\,1-\alpha} \tag{3.24}$$

with $\chi^2_{m-1,\,1-\alpha}$ denoting the $(1-\alpha)$-quantile of the chi-square distribution with $m-1$ degrees of freedom. Consequently, the parameter ρ is defined as

$$\rho = \frac{\phi''(1)}{2M} \chi^2_{m-1,\,1-\alpha}, \tag{3.25}$$

which depends on the sample size M, the number of grid points m, and the significance level α.

Building upon this characterization of candidate distributions, we now focus on approximating the worst-case expectation, which corresponds to the inner problem of Eq. (3.18). To this end, we discretize the probability density function (PDF) of the KPI. Let $L, U \in \mathbb{R}$ with $L < U$ be the lower and upper bounds of the KPI over the feasible set $\mathcal{Q}$ of the uncertain parameter $\mathbf{Q}$:

$$L = \inf_{\mathbf{Q} \in \mathcal{Q}} KPI(x, \mathbf{Q}), \qquad U = \sup_{\mathbf{Q} \in \mathcal{Q}} KPI(x, \mathbf{Q}). \tag{3.26}$$

The interval $[L, U]$ is uniformly partitioned into w subintervals of length $\Delta = (U - L)/w$. The grid points $(g_i)_{1 \le i \le w}$ are placed at the centers of these subintervals, i.e., $g_i = L + (i - \frac{1}{2})\Delta$, as illustrated in Figure 4. The continuous PDF F is then approximated by the discrete vector $\hat{\mathbf{F}} = (\hat{F}_i)_{1 \le i \le w}$, where $\hat{F}_i \approx F(g_i)$.

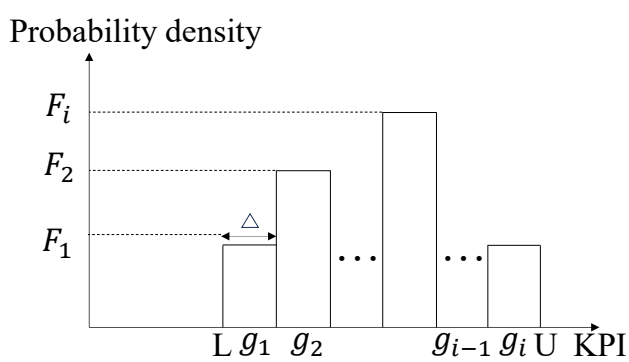

Figure 4: Discrete approximation of the PDF of KPI.

The probability mass at grid point g_i is given by $p_i = \hat{F}_i \Delta$, which approximates the integral of the PDF over the i-th subinterval using the rectangle rule (midpoint rule). These probability

masses satisfy $\sum_{i=1}^{w} p_i = 1$ and $p_i \geq 0$. The uncertainty set $\mho(x)$ imposes additional constraints on the shape of the PDF, which translate into box constraints on the probability masses:

$$\underline{p}_i \leq p_i \leq \overline{p}_i, \quad \forall i, \tag{3.27}$$

where $\underline{p}_i$ and $\overline{p}_i$ are the minimum and maximum feasible values of p_i derived from $\mho(x)$.

Consequently, the inner problem in Eq. (3.18) can be approximated by the following linear program (LP):

$$\max_{D \in \mho(x)} \mathbb{E}_D[KPI(x, \mathbf{Q})] \approx \max_{\mathbf{p}} \left\{ \sum_{i=1}^{w} g_i p_i \ : \ \sum_{i=1}^{w} p_i = 1, \ p_i \geq 0, \ \underline{p}_i \leq p_i \leq \overline{p}_i, \ \forall i \right\} \tag{3.28}$$

3.3.2 Selection of ϕ-divergence function

The selection of an appropriate ϕ-divergence function is a critical step, which should be guided by the characteristics of the available data (Bayraksan and Love, 2015; Zhu et al., 2018). These adjustments are characterized by two classification rules: suppression and popping.

Definition 3.3 (Suppression)**.** *The ability to assign zero or reduced probability to scenarios that are present in the empirical sample but are deemed unreliable.*

Definition 3.4 (Popping)**.** *The ability to assign positive probability to scenarios that are* not *observed in the empirical sample.*

Specific instances of these divergence functions are summarized in Table A.1, with explanatory notes provided subsequently. It is important to note that this classification is not unique; alternative frameworks could be applied depending on the modeling context.

Whether suppression is permissible depends on the quality of the historical data. Suppression Allowed: When prior data are of poor quality, e.g., collected over short durations, from uncensored road segments, or under atypical conditions such as severe weather or accidents, suppression prevents the model from overfitting to sparse or unrepresentative samples. The optimization then concentrates on more trustworthy observations. Suppression Disallowed: If the historical data are abundant and of high quality, all observed scenarios should be retained to avoid discarding valuable empirical information. Disallowing suppression yields a conservative model that fully exploits the available data.

Whether popping is beneficial depends on the availability of qualitative information beyond the quantitative sample. Popping Allowed: Popping is desirable when qualitative sources, e.g., expert opinions, surveys, or domain knowledge, suggest the existence of plausible scenarios not captured by quantitative data (such as GPS traces or sensor readings). Enlarging the support of the distribution expands the family of candidate probability models and mitigates the risk of underestimating uncertainty. Popping Disallowed: If no theoretical or qualitative basis supports the existence of unobserved scenarios, or if decision makers intend to adhere strictly to the empirical distribution, popping should be disallowed. The support is then confined to the observed sample.

The Kullback-Leibler divergence in Table A.1 is selected in this paper because it rigorously rejects distributions exhibiting "popping" (assigning probability to unobserved values). This ensures conservative, empirically supported models that control tail risks and prevent over-optimistic extrapolation.

3.3.3 DRO under predetermined controls

At the pre-tactical level, the DRO framework informs fleet-size decisions prior to daily operations, using demand forecasts as input. Constructing this formulation first requires an initial uncertainty set, which is empirically built from M days of historical trip requests following the procedure in Section 3.3.1.

The monitoring cost differential, the extra operational cost incurred when instrumented vehicles are rerouted from passenger-seeking to sensing tasks, is treated as a random variable influenced by latent, interrelated factors regarding demand fluctuations. Instead of assuming a parametric distribution, we adopt a nonparametric, data-driven representation using the bivariate structure:

$$\boldsymbol{\Xi}^k = \left(\xi_t^k, \zeta_t^k\right)_{t \in T}, \quad k = 1, \ldots, M, \tag{3.29}$$

where ξ_t^k denotes the baseline monitoring cost during interval t on day k, and ζ_t^k is an auxiliary cost modifier that depends on the operational context (Binzhou Yang et al., 2026) [1]. The collection

$$\mathfrak{D} = \{\boldsymbol{\Xi}^1, \boldsymbol{\Xi}^2, \ldots, \boldsymbol{\Xi}^M\}$$

consists of M i.i.d. realizations of an unspecified random vector $\mathbf{Q}$, providing the empirical basis for the subsequent distributionally robust treatment.

To evaluate the objective in Eq. (3.18) for a candidate instrumented fleet size N_1, we first retrieve historical trip records covering the designated sensing horizon. The enhanced A* routing protocol (Section 3.2) is then applied to simulate per-interval monitoring costs, yielding m independent KPI realizations, each representing the total monitoring cost incurred by the mixed-fleet ride-hailing system. A linear programming routine subsequently computes the worst-case expectation from this empirical KPI sample, which serves as the robustness-adjusted performance metric. Since the set of feasible fleet sizes is finite, the optimal configuration is identified by direct enumeration, for higher-dimensional decision spaces, metaheuristic methods (e.g., genetic algorithms, simulated annealing) are employed to maintain computational tractability.

Remark 3.5. *A key methodological feature of this pipeline is that it omits explicit behavioral or structural assumptions about DS ride-hailing market dynamics (e.g., trip generation). Instead, this information is incorporated via two complementary mechanisms: an empirically derived uncertainty set, and trajectory-level realism from the A* routing heuristic. This approach is analogous to Monte Carlo simulation. Rather than exhaustively modeling stochastic primitives, we simulate system realizations directly from historical data. The resulting empirical distribution of the objective is then embedded into the distributionally robust optimization (DRO) framework without parametric intermediaries.*

3.3.4 DRO under adaptive controls based on rolling horizon

The DRO-based pre-tactical planning model in Section 3.3.3 produces decisions from day-ahead demand forecasts that remain static throughout the operating day, offering no adaptability to real-time updates. In practice, however, demand predictions are continually refined at shorter look-ahead times (LAT), e.g., hourly, yielding rolling forecasts that are more accurate and inherently capture real-time factors, such as weather, that affect ride demand. To harness these progressively improved estimates, we adopt a rolling horizon framework that reapplies the

[1] In this paper, the auxiliary cost modifier aligns with the subsidy incentive cost item, which is designed to incentivize instrumented drivers to continuously accept orders.

DRO methodology from Section 3.3.3 at each LAT-aligned interval with minimal modifications, allowing each decision to incorporate the latest forecast. The LAT itself is not fixed, it embodies a context-dependent trade-off between forecast precision and computational cost (e.g., DRO solution time) and can therefore be tailored to diverse operational environments.

4 Numerical test

This section presents a case study conducted in the Longquanyi District of Chengdu. It begins with a description of the trip demand configuration, simulation initialization, taxi operation modes, distribution of monitoring POIs, and the optimization method, followed by implementation details in Section 4.1. Subsequently, Section 4.2 presents the results of the deterministic, DRO, and DRO with rolling horizon frameworks. Section 4.3 shows the simulation results of key operational performance indicators. Finally, the performance of monitoring timeliness for POIs and the enhanced A* drive-by sensing routes are discussed in Sections 4.4 and 4.5, respectively.

Trip Demand Configuration. Trip demand is characterized using historical completed trip data collected between 8:00 and 12:00 from August 1 to December 31, 2021. To capture the influence of demand patterns on system performance, multiple demand scenarios are constructed. Demand Scenario 1 serves as the baseline and is derived directly from actual completed trips. Two additional scenarios (Demand Scenarios 2 and 3) are synthetically generated by progressively increasing the proportion of remote trips, defined as trips ending in areas with low local demand, while keeping the total number of trip requests constant at approximately 144 per hour. Thus, the three scenarios differ exclusively in the spatial distribution of trip demand, as illustrated in Figure 5. Induced demand and unmet demand are not considered in this study.

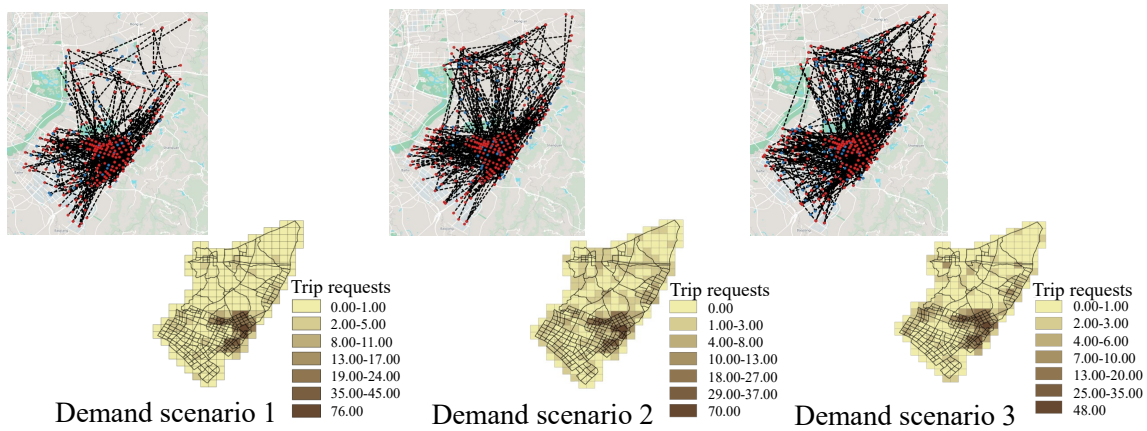

Figure 5: The three demand scenarios, with increasing percentage of remote order number. The origin is marked in red, and the destination is marked in blue.

Simulation Initialization. The simulation covers a four-hour period, divided into four 1-hour sensing intervals. Each sensing interval consists of 18 decision epochs, each lasting 200 seconds. At the start of each epoch, the ride-hailing platform collects real-time trip requests and the locations of vacant instrumented taxis. At the beginning of each simulation run, all taxis are randomly positioned within the road network. Vacant taxis initially cruise toward areas with higher trip request densities until they receive ride assignments.

Taxi Operation Mode. All taxis operate at a constant speed of 35 km/h. At each decision

epoch, the platform executes the matching mechanism described in Section 3.1.2, generating matched pairs and optimal routes. The system state is propagated to the subsequent epoch to ensure continuity in the dynamic simulation. Vacant taxis continue cruising when no ride assignments are received.

Distribution of Monitoring Points. A total of 85 monitoring points of interest (POIs) are randomly selected as reference locations, as depicted in Figure 6.

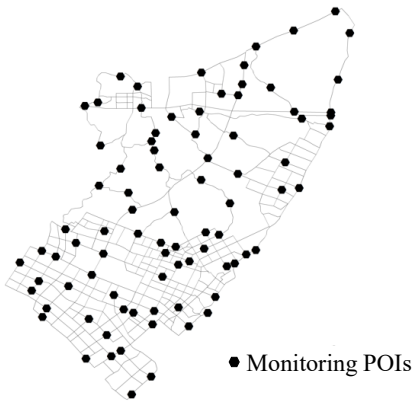

Figure 6: Monitoring POIs in Longquanyi District.

Optimization Methods. Depending on data availability and the scope of optimization methods, three variants of the proposed framework are implemented. The deterministic approach applies pre-determined control strategies without accounting for uncertainty. The DRO-based approach (Section 3.3.3) also adopts pre-determined control but explicitly considers demand uncertainty. The DRO_{RH} approach (Section 3.3.4) incorporates adaptive control with a rolling horizon scheme, wherein a one-hour demand prediction is provided at the beginning of each time window. All methods are evaluated using the 85 randomly selected monitoring POIs.

4.1 Implementation details

The proposed matching procedure, executed within each decision epoch, is implemented using the following techniques and specifications (see Figure 1 for details):

1. Matching Radius: A search radius of 2 km is applied for driver-rider matching. Consequently, driver-rider pairs separated by more than 2 km are excluded from the matching process.

2. Step 1 (Sensing-Optimized Matching): In Step 1 of Figure 1, only the service leg of a matched trip (excluding the pick-up phase) contributes to the sensing externality objective in (3.4). This design is intended to avoid excessively long pick-up distances incurred by the pursuit of sensing gains. Under the constraint of maximizing the sensing externality, each rider is matched to the nearest available driver to minimize customer wait time.

3. Step 2 (Non-Instrumented Taxi Matching): We maximize the number of matches between non-instrumented taxis and riders. This step thereby improves the overall matching rate after Step 1.

4. Step 3 (POI Monitoring Task Matching): With the maximum number of matches between vacant instrumented taxis and monitoring POIs as the primary objective to fulfill more monitoring tasks, we then maximize utility time-efficiency. Note that if a POI was already included in the route of a pair matched in Step 1, it is considered a completed monitoring task and is excluded from Step 3.

4.2 Results of Deterministic, DRO, and DRO with rolling horizon frameworks

Table 2 summarizes the training and testing performance of the Deterministic, DRO, and DRO_{RH} models in terms of monitoring cost. The Design Key Performance Indicator (Design KPI) presented in this table is defined as the average monitoring cost per instrumented taxi per unit time, which incorporates both the operational cost of the enhanced A* drive-by sensing route service policy and the subsidy incentives provided to the instrumented taxis.

The "Optimal size" column lists the optimal fleet size (in vehicles) identified by each method. The "Design KPI" column reports the actual performance metric when the optimal fleet size is applied to the realized demand data, as opposed to the predicted demand used for optimization.

Table 2: Training and testing results of the three optimization frameworks

Testing time	Demand distribution	Optimization method	Instrumented taxis fleet size						Optimal size (vehicles)	Design KPI (CNY/h/vehicle) for the optimal size
			10	20	30	40	50	60		
8:00-12:00, collected from 1 Aug to 31 Dec, 2021	Demand Scenario 1	Deterministic	50.935	23.999	15.341	11.633	8.374	6.963	60	6.963
		DRO	36.053	18.932	12.590	9.227	6.815	4.759	60	4.759
		DRO_{RH}	35.717	18.077	11.585	8.321	6.281	5.137	60	5.137
	Demand Scenario 2	Deterministic	45.186	25.083	14.388	10.452	8.207	6.715	60	6.715
		DRO	33.629	18.914	11.691	8.146	6.623	5.271	60	5.271
		DRO_{RH}	32.416	18.330	10.924	7.433	5.917	4.854	60	4.854
	Demand Scenario 3	Deterministic	40.938	26.171	16.216	11.147	8.252	6.057	60	6.057
		DRO	33.153	18.603	12.167	8.847	6.348	4.995	60	4.995
		DRO_{RH}	31.967	17.343	11.142	7.644	5.744	4.297	60	4.297

Specifically, across three demand scenarios with fleet sizes ranging from 10 to 60 vehicles, DRO_{RH} achieves superior performance in 17 out of 18 comparisons (94.4%), with an average KPI reduction of 0.3–1.3 CNY/h/vehicle compared to the standard DRO approach. The advantage is most pronounced under high-demand conditions (Demand Scenario 3), where DRO_{RH} consistently outperforms DRO across all fleet sizes with KPI improvements of up to 1.26 CNY/h/vehicle at 20 vehicles (18.603 vs. 17.343 CNY/h/vehicle). Notably, the only exception occurs in the lowest demand scenario (Demand Scenario 1) with the largest fleet size (60 vehicles), where DRO slightly outperforms DRO_{RH} by a marginal 0.378 CNY/h/vehicle (4.759 vs. 5.137 CNY/h/vehicle)—a mere 7.4% difference. This single counterexample actually reinforces the method's validity, as it aligns with theoretical expectations: when the fleet size is sufficiently large relative to demand, temporal demand variations are smoothed out, making the pooled estimation approach (DRO) marginally more efficient. These results demonstrate that DRO_{RH} effectively captures time-varying demand patterns under realistic resource constraints, validating its robustness for practical implementation.

The results indicate that the DRO_{RH} model outperforms the other two approaches. It achieves this by dynamically adjusting the fleet size (between 10 and 60 vehicles) in response to updated travel demand over time. This evaluation demonstrates the effectiveness of the proposed controls under real-world uncertainty. The DRO approach mitigates the impact of

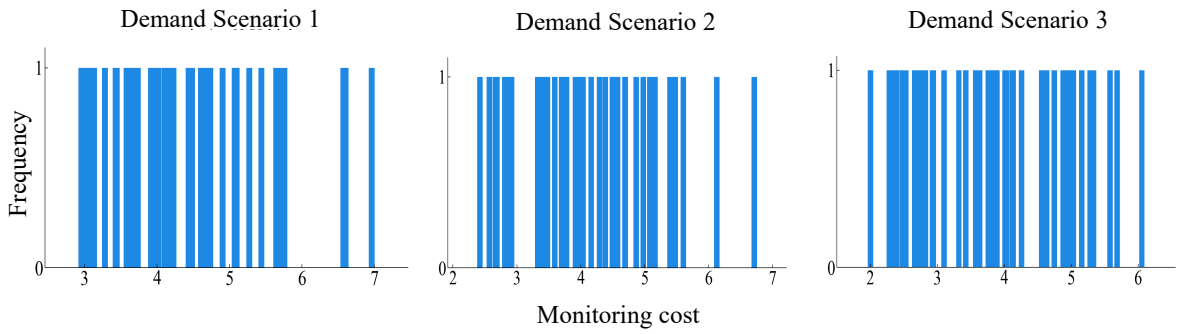

Figure 7: Histograms of the "Design KPI" under the optimization method of DRO_{RH} approach, based on results from 10 simulation runs across three demand scenarios. The X-axis represents the per-unit-time monitoring cost per instrumented taxi (CNY/h/vehicle), and the Y-axis shows the corresponding frequency (count) in the simulation tests.

outliers in a tunable manner through the selection of α. This adjustability enables a less conservative interpretation of uncertainties, which in turn leads to superior system performance, as evidenced in Figure 7.

4.3 Simulation results on operational performance KPIs

This subsection evaluates the operational performance in terms of three key performance areas (KPAs) and five key operational performance indicators (abbreviated as OP-KPIs):

- **Level of service**: (1) *Matching rate*, which is the percentage of riders that are matched to drivers; (2) *Average wait time*, which is the averaged pick-up times τ_{dr} of matched pairs.
- **Sensing externality**: (3) *Sensing utility* Γ, which is given in Eq. (3.1); (4) *Grid coverage rate*, which is the average % of grids covered at least once in an hour.
- **Monitoring capability:** (5) *Monitoring completion rate*, which is the total completion rate of overall monitoring POIs.

Figure C.1 through Figure C.3 present the operational performance across three Demand Scenarios for fleet sizes ranging from 10 to 60 vehicles. The evaluated performance metrics include matching rate (%), and average wait time (min), the sensing utility (Γ), percentage of grids covered per hour, monitoring completion rate (%). Based on 10 independent simulation runs, the following observations are drawn from the figures:

1. The level of service, characterized by matching rate and average wait time, varies with the instrumented fleet size. Demand Scenario 3 shows the lowest matching rate, as drivers tend to cruise in areas with concentrated order density. As shown in Figure 1, the multi-objective optimization of fixed prioritization strategies leads to rigid resource allocation. In a dynamic environment with arriving trip requests and monitoring POIs, the increase in instrumented taxis leads to periodic conflicts between the sensing objective and the customer-matching objective, resulting in non-monotonic oscillatory variations in the matching rate.

2. Demand Scenario 3, with the highest proportion of remote orders, also exhibits the highest average wait time. The average wait time shows a non-monotonic trend, initially increasing and then decreasing with fleet size, which stems from the optimization mechanism illustrated in Figure 1. With fewer instrumented taxis, the platform prioritizes sensing maximization, leading to longer customer wait times. As the fleet expands beyond a certain threshold, sufficient instrumented taxis are assigned under this objective to serve a significant share of travel demand. This increase in instrumented taxis alleviates the conflict between sensing and service objectives, allowing the subsequent customer wait time minimization module to assign nearer taxis more effectively, thereby reducing the overall average wait time.

3. The sensing externality (encompassing sensing utility and grid coverage rate) and monitoring capacity (indicated by monitoring completion rate) both improve as the size of instrumented taxi fleets increases. Demand Scenario 3 exhibits higher sensing utility and grid coverage rate, attributable to its higher proportion of remote orders.

4.4 Monitoring timeliness of POIs

Using the dispatch cycle from 8:00 to 12:00 as a reference, we statistically analyze the scheduled monitoring times of 85 POIs, as shown on the horizontal axis of Figure 8. To verify that deploying vacant instrumented taxis for POI monitoring can achieve timely and effective monitoring coverage and data collection in blind spots, we examine the monitoring timeliness of these POIs under two modes: with active sensing and without active sensing. The following conclusions are drawn:

- The blue dots represent the scheduled monitoring times of POIs. The darker the color, the greater the number of associated POIs. The red dots represent POIs that are not monitored within the calculated time domain. This situation occurs only in the "without active sensing" mode.

- The diagonal line, where the x-coordinate equals the y-coordinate for every point on it, is defined as the ideal monitoring line. If a point defined by the actual monitoring time (vertical axis) and the scheduled monitoring time (horizontal axis) falls exactly on this line, it indicates strong timeliness for that POI. As can be seen from Figure 8, the actual POI monitoring times in the "without active sensing" mode are scattered more in the upper-left area above the ideal monitoring line rather than on the line itself. The timeliness of the "with active sensing" mode is better than that of the "without active sensing" mode.

- When the order distribution is more balanced, there are fewer unmonitored POIs in the "without active sensing" mode. This is because POIs widely distributed across the measurement area (as shown in Figure 6) are more likely to be covered and monitored by fleets of instrumented taxis that are occupied (i.e., serving passengers).

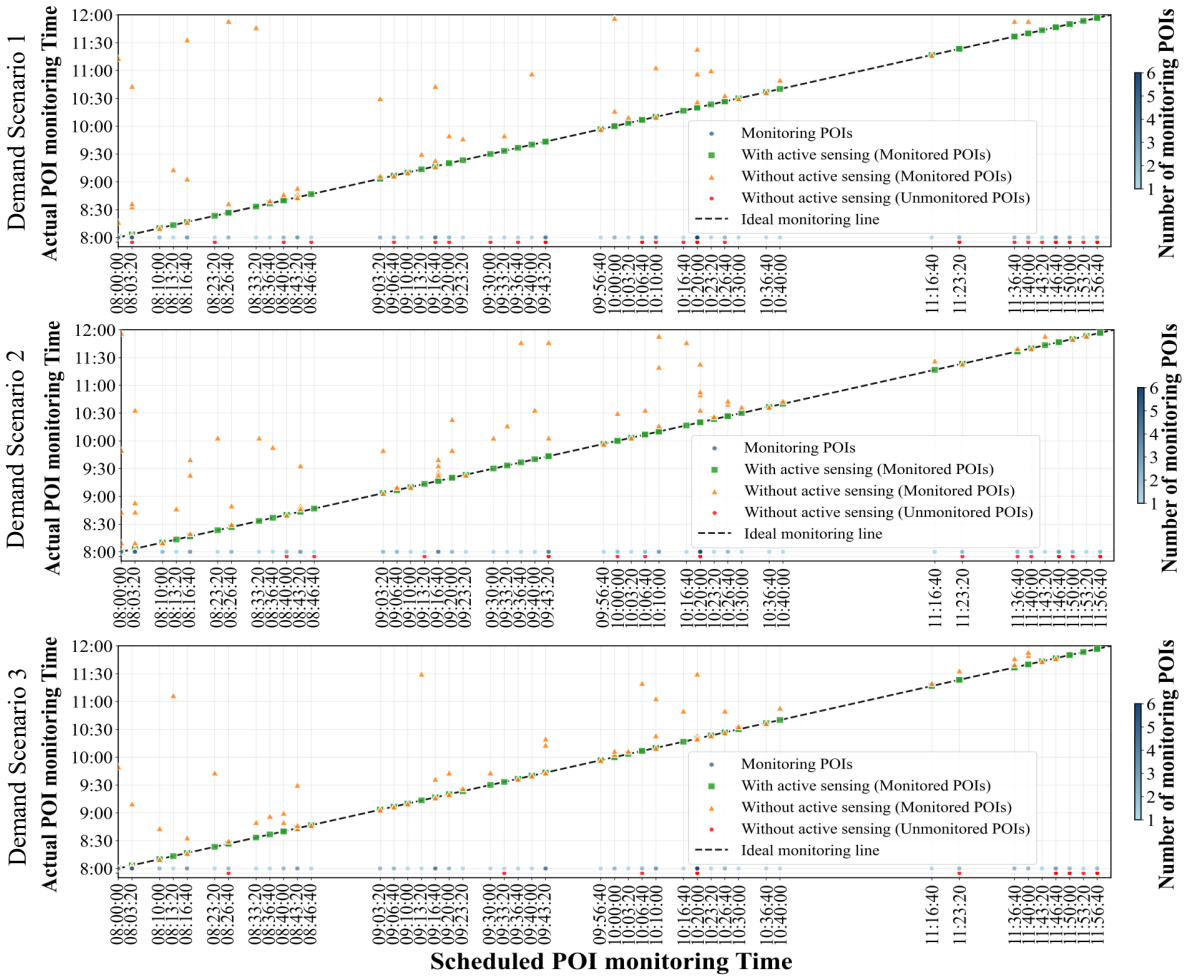

Figure 8: Monitoring timeliness of POIs under Demand Scenario 1, 2 & 3 (with regards to 60 instrumented taxis).

4.5 Enhanced A* drive-by sensing routes

With reference to Table 2, a fleet size of 60 instrumented taxis (N=60) is examined across Demand Scenarios 1, 2, and 3 for illustrative purposes. Figure 9 depicts all enhanced A* sensing routes generated by vacant instrumented taxis during time period T following the proposed algorithm. Further algorithmic details are provided in Tables B.1 and B.2.

The following observations are derived:

- The origin of each route is defined as the initial position of a vacant instrumented taxi when dispatched for POI monitoring, while the destination is the target monitoring POI assigned to it. As shown in Figure 9, the number of distinct destinations is smaller than the total number of monitoring POIs shown in Figure 6. This discrepancy occurs because some monitoring tasks are fulfilled as a byproduct of regular trip assignments to instrumented taxis.

- The POI monitoring route is defined as the optimized paths determined by the enhanced A* algorithm to accomplish a sensing task. The distribution of travel demand and the spatial dispersion of monitoring POIs exert a significant influence on these routes of

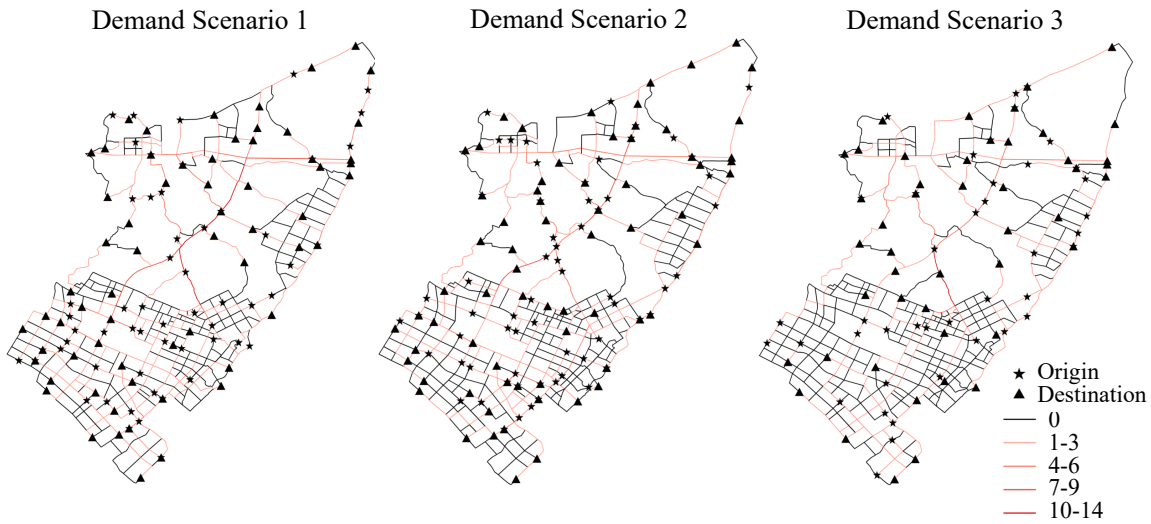

Figure 9: Enhanced A* drive-by sensing routes under Demand Scenario 1, 2 & 3 (with regards to 60 instrumented taxis).

vacant instrumented taxis, which in turn affects the visiting frequencies across different network nodes and edges, as visually summarized in Figure 9.

- The proposed DRO model quantifies the monitoring cost by applying a unit cost of 1.5 CNY/km to the total distance traveled by vacant instrumented taxis along their assigned POI monitoring routes. This formulation aligns with the comprehensive cost framework, which integrates both the operational expenditures for POI monitoring and the subsidy incentives allocated to the entire instrumented taxi fleet.

5 Discussion

The current DS ride-hailing market, which comprises mixed instrumented taxi fleets, operates under a conventional deterministic monitoring pattern. This approach leads to highly inefficient operations, primarily due to the excessive monitoring costs incurred by POI monitoring demand.

The framework proposed in this study serves as a foundational component for a novel mixed DS ride-hailing market design, incorporating an enhanced A* drive-by sensing route policy. Unlike the static and disjointed conventional approach, the proposed framework explicitly accounts for the dynamic fluctuations in POI monitoring, which are driven by various random variables with regard to the market' uncertain ride demand. Furthermore, by optimizing the selection of instrumented taxi fleets according to the heterogeneous spatio-temporal distribution of travel demand, this framework enhances the resource efficiency of the DS ride-hailing market.

Within the paradigm of the enhanced A* drive-by sensing policy, and given the current absence of methods for evaluating dynamic monitoring route effectiveness, even the least sophisticated variant of our framework (the deterministic model) yields a feasible monitoring cost scheme and demonstrates potential for improving upon the status quo. The DRO model and its rolling-horizon variant achieve superior performance against the Design KPI. The dis-

tributionally robust technique is particularly effective at managing highly volatile dynamic demand, delivering robust and reliable outcomes. The identified monitoring patterns are validated using ten historical datasets across three distinct demand distributions. Therefore, the validated framework facilitates cost optimization by translating unimpeded POI monitoring demand into quantifiable costs under the enhanced A* drive-by sensing route policy.

The automation of the proposed framework is anticipated to alleviate the operational workload within the DS ride-hailing market, substantially reducing specific tasks such as route planning for vacant instrumented taxis and monitoring cost optimization. Furthermore, the framework's robustness, demonstrated through the DRO approach, allows it to effectively accommodate daily ride demand variability and uncertainty. Although developed and validated for the Longquanyi District, the methodology is readily transferable to other regions with POI monitoring requirements. It should be noted, however, that implementation may shift the operational focus from active sensing to passive sensing, a transition with significant practical implications.

6 Conclusion

This paper introduces a DS ride-hailing market that incorporates mixed instrumented taxis to address the demand for tasks monitoring. In contrast to existing approaches, the proposed methodology accounts for the uncertainty arised from uncertain ride demand. It serves the dual purposes of POI monitoring and the robust assessment of monitoring costs. The methodology is summarized as follows:

- An enhanced A* drive-by sensing route service policy is formulated to coordinate vacant instrumented taxis with the monitoring of POIs, within the context of a ride-hailing market operation that utilizes mixed instrumented fleets.
- The DRO technique is employed to address ambiguities in the underlying distributions of complex, correlated random variables. This approach simultaneously tackles challenges related to insufficient data availability and limited data granularity.

To rigorously validate and quantify the efficacy of the proposed framework, extensive simulations are conducted based on a real-world drive-by air quality monitoring scenario. The results demonstrate that:

1. Under the enhanced A* drive-by sensing route service policy, the DRO_{RH} technique demonstrates superior performance compared to the standard Deterministic and DRO techniques. Its advantage lies in prioritizing the reduction of conservatism, as evidenced by the evaluation results of the monitoring cost KPI. For the DRO_{RH} optimization method, the optimal sensor deployment is 60 fleets across all demand scenarios for the specified POIs. Demand Scenario 1, which has a relatively unbalanced spatial trip distribution, exhibits the highest monitoring cost per unit time per vehicle.
2. The proposed operational framework for the DS ride-hailing platform, integrating optimal sensor deployment and the enhanced A* drive-by sensing route, achieves the anticipated performance in both service quality and sensing capabilities. Service quality is measured by the matching rate and average wait time, while sensing capabilities are evaluated through sensing utility, percentage of grids covered per hour, and monitoring completion rate.

3. Planning vacant instrumented taxis to monitor POI makes data collection from monitoring blind spots more timely. The enhanced A*-based drive-by sensing routes between vacant instrumented taxis and monitoring POIs are incorporated into the platform's POI monitoring cost at a rate of 1.5 CNY/km. In addition to these dedicated routes, POI monitoring may also be completed indirectly when instrumented taxis fulfill actual customer trip requests.

Based on travel demand data and targeted POIs, the DRO framework is recommended as an effective guideline for monitoring cost optimization, providing strategic direction for the long-term operation of ride-hailing markets with mixed instrumented fleets. An important extension of the current framework involves incorporating sensor failures and heterogeneous sensor types into the model. Such challenges could be addressed using the DRO methodology presented in this study.

Declaration of competing interest

The authors declare that they have no known competing financial interests or personal relationships that could have appeared to influence the work reported in this paper.

CRediT authorship contribution statement

Binzhou Yang: Writing – original draft, Visualization, Methodology, Investigation, Formal analysis, Conceptualization, Resources, Visualization. Bin Shuai: Supervision, Resources. Minhao Xu: Project administration, Funding acquisition. Boyang Du: Visualization.

Acknowledgement

We thank Dr. Lei Yang for the helpful discussions. This work is partly supported by the China Postdoctoral Science Foundation (2025MD784117), the Tianyou Postdoctoral Science Foundation of Lanzhou Jiaotong University, China (LJTYBH-2026002).

Appendix A ϕ-divergence

The adjoint and conjugate of ϕ-divergence for some specific choices.

Table A.1: Some specific choices of ϕ-divergence and their adjoint and conjugate

ϕ-divergence	$\phi(u)$	$I_\phi(p,q)$	popping	suppression
Kullback-Leibler	$\phi_{kl}(u) = ulogu - u + 1$	$\sum p_j log\frac{p_j}{q_j}$	×	✓
Burg entropy	$\phi_b(u) = -logu + u - 1$	$\sum q_j log\frac{q_j}{p_j}$	✓	×
J-divergence	$\phi_j(u) = (u-1)logu$	$\sum(p_j - q_j)log\frac{p_j}{q_j}$	×	×
χ^2-divergence	$\phi_c(u) = \frac{1}{u}(u-1)^2$	$\sum \frac{(p_j-q_j)^2}{p_j}$	✓	×
Modified χ^2-divergence	$\phi_{mc}(u) = (u-1)^2$	$\sum \frac{(p_j-q_j)^2}{q_j}$	×	✓
Hellinger distance	$\phi_h(u) = (\sqrt{u}-1)^2$	$\sum(\sqrt{p_i} - \sqrt{q_i})^2$	✓	✓
Variation distance	$\phi_v(u) = \lvert u-1 \rvert$	$\sum \lvert p_i - q_i \rvert$	✓	✓

Appendix B The enhanced A* drive-by sensing route

The POI monitoring routings for a single vacant instrumented taxi and for multiple vacant instrumented taxis at dual spatial scales are shown in Table B.1 and Table B.2, respectively.

Table B.1: Executing a N-route and corresponding G-route

Algorithm1	
Input	Starting node $\tau_1 \in g_1$, corresponding monitoring POI $\tau \in \mathcal{N}$.
Step 1	Apply the modified A* algorithm to find the shortest path $p^* = (\tau_1, ..., \tau_m)$ and corresponding N-route $\bar{\kappa}(\tau_1; \kappa_G)$.
Step 2	Calculate the actual G-route $G_{\bar{\kappa}(\tau_1;\kappa_G)}$ traversed by $\bar{\kappa}(\tau_1; \kappa_G)$.
Step 3	Calculate $\varphi(d\tau)$ and matching pair $x_{d\tau}$ combined with Eqs. (3.12) - (3.16) .
Output	Matching pair $x_{d\tau}$, N-route $\bar{\kappa}(\tau_1; \kappa_G)$, G-route $G_{\bar{\kappa}(\tau_1;\kappa_G)}$.

Table B.2: Multi-vehicle routing for discrete time window t

Algorithm 2	
Input	Vacant instrumented taxis $n = 1...n^D$ and monitoring POI $\tau \in \mathcal{N}$, maximum iteration limit max_iter.
Initialize	Set $k = 1$.
Step 1	Apply Algorithm 1 to the vacant instrumented taxis $n = 1...n^D$ and monitoring POI $\tau \in \mathcal{N}$.
Step 2	Adjust routing solutions. For $n = 1, ..., n^D$:
Step 2a	If the n-th vacant instrumented taxi has formed a monitoring POI matching pair, the pair is dissolved and the coverage utility contributed by the n-th vacant instrumented taxi is removed;
Step 2b	Apply the Algorithm 1 to the n-th vacant instrumented taxi, if the new solution yields higher utilities than the current solution, then accept the new solution; otherwise, retain the current solution; set k=k+1;
Step 3	If no solutions are updated for any of the vacant instrumented taxis or k=max_iter, terminate the Algorithm 2; otherwise, go to Step 2.
Output	Routing solutions $R^D = R_1^D, ..., R_{n^D}^D$ for n^D vacant instrumented taxis.

Appendix C Operational performance figures

In line with Section 4.3, the operational performance across three demand scenarios for fleet sizes of 10-60 vehicles is presented in Figures C.1–C.3, including level of service, sensing externality and monitoring capability. In particular, building upon prior research (Yang et al., 2025), we have incorporated simulation tests of monitoring capability in Figure C.3.

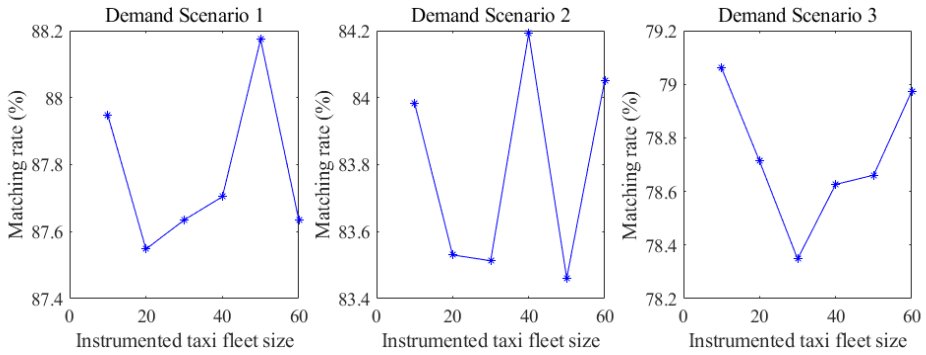

Figure C.1: Matching rate under different demand scenarios and instrumented taxi fleet size.

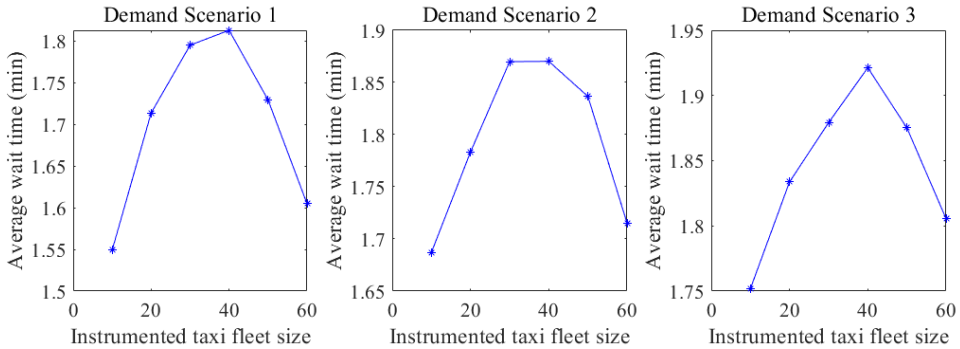

Figure C.2: Average wait time under different demand scenarios and instrumented taxi fleet size.

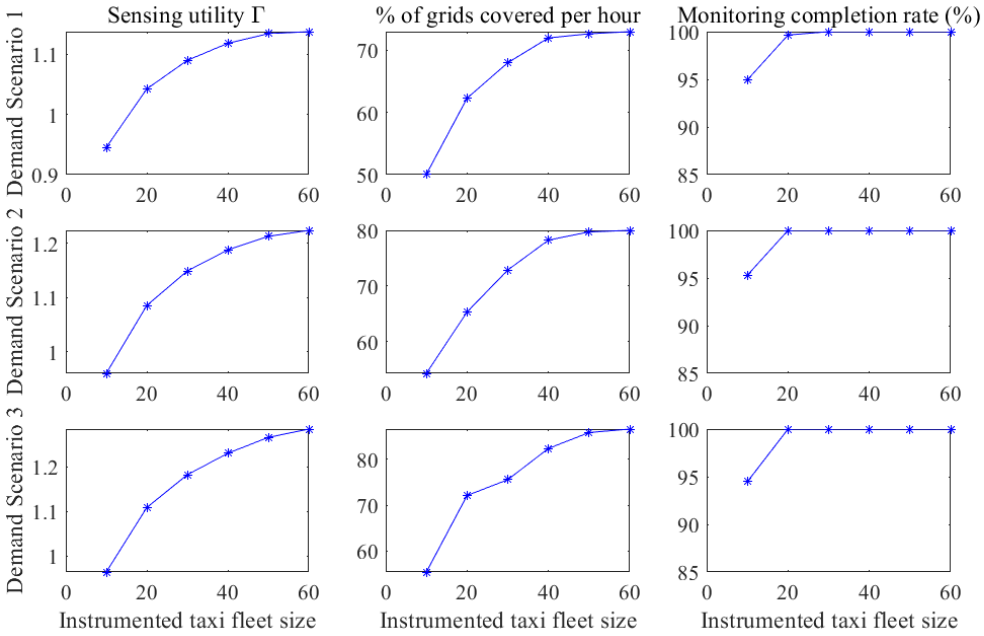

Figure C.3: The sensing externality and monitoring capacity under different demand scenarios and instrumented taxi fleet size.

References

Ahipasaoglu, S.D. , Meskarian, R. , Magnanti, T.L. , & Natarajan, K. (2015). Beyond normality: a cross moment-stochastic user equilibrium model - sciencedirect. Transportation Research Part B: Methodological, 81, 333-354.

Ali, J., & Dyo, V. (2017). Coverage and mobile sensor placement for vehicles on predetermined routes: a greedy heuristic approach. In Proceedings of the 14th International Joint Conference on e-Business and Telecommunications (ICETE 2017) - WINSYS (pp. 83-88). SciTePress.

Asprone, D., Di Martino, S., Festa, P., & Starace, L. L. L. (2021). Vehicular crowd-sensing: a parametric routing algorithm to increase spatio-temporal road network coverage. International Journal of Geographical Information Science, 35(9), 1876-1904.

Ardestani-Jaafari, A., & Delage, E. (2017). The Value of Flexibility in Robust Location–Transportation Problems. Transportation Science 52(1):189-209.

Binzhou Yang, Chuandang Zhao, & Ke Han. (2026). Pricing and equilibrium of ride-hailing market with mixed drive-by sensing fleets. Paper presented at the 105th Annual Meeting of the Transportation Research Board, Washington, DC.

Bayraksan, G. , Love, D.K. , 2015. Data-driven stochastic programming using phi-divergences. In: The Operations Research Revolution. INFORMS, pp. 1–19 .

Ben-Tal, A., Den Hertog, D., De Waegenaere, A., Melenberg, B., & Rennen, G. (2013). Robust solutions of optimization problems affected by uncertain probabilities. Management Science, 59(2), 341-357.

Bock, F., Attanasio, Y., & Di Martino, S. (2017). Spatio-temporal road coverage of probe vehicles: a case study on crowd-sensing of parking availability with taxis. In Societal Geoinnovation: Selected papers of the 20th AGILE conference on Geographic Information Science, pp. 165-184. Springer International Publishing.

Bonola, M., Bracciale, L., Loreti, P., Amici, R., Rabuffi, A., & Bianchi, G. (2016). Opportunistic communication in smart city: Experimental insight with small-scale taxi fleets as data carriers. Ad Hoc Networks, 43, 43-55.

Cruz, P., Couto, R.D., Costa, L.H., Fladenmuller, A., & Amorim, M.D. (2020). A delay-aware coverage metric for bus-based sensor networks. Computer Communications, 156, 192-200.

Cruz, P., Couto, R.D., Costa, L.H., Fladenmuller, A., & de Amorim, M. (2020). Per-vehicle coverage in a bus-based general-purpose sensor network. IEEE Wireless Communications Letters, 9, 1019-1022.

Chen, X., Xu, S., Han, J., Fu, H., Pi, X., Joe-Wong, C., Li, Y., Zhang, L., Noh, H.Y., & Zhang, P. (2020). Pas: Prediction-based actuation system for city-scale ridesharing vehicular mobile crowdsensing. IEEE Internet of Things Journal, 7(5), 3719-3734.

Chen, Y., Lv, P., Guo, D., Zhou, T., & Xu, M. (2017). Trajectory segment selection with limited budget in mobile crowd sensing. Pervasive and Mobile Computing, 40, 123-138.

Chen, X. , Sim, M., & Sun, P. (2007). A robust optimization perspective on stochastic programming. Operations Research, 55(6), 1058-1071.

Delage, E. , & Ye, Y. (2010). Distributionally robust optimization under moment uncertainty with application to data-driven problems. Operations Research, 58(3), 595-612.

Fan, G., Jin, H., Liu, Q., Qin, W., Gan, X., Long, H., Fu, L., & Wang, X. (2021). Joint scheduling and incentive mechanism for spatio-temporal vehicular crowd sensing. IEEE Transactions on Mobile Computing, 20, 1449-1464.

Gao, Y., Dong, W., Guo, K., Liu, X., Chen, Y., Liu, X., Bu, J., & Chen, C. (2016). Mosaic: A low-cost mobile sensing system for urban air quality monitoring. IEEE INFOCOM 2016 - The 35th Annual IEEE International Conference on Computer Communications (pp: 1-9).

Goh, J. , & Sim, M. (2010). Distributionally robust optimization and its tractable approximations. Operations Research, 58(4-part-1), 902-917.

Guo, S., Qian, X., Dasgupta, S., Rahman, M., & Jones, S. (2022). Sensing and monitoring of urban roadway traffic state with large-scale ride-sourcing vehicles. The Rise of Smart Cities, 551-582.

Guo, S., & Qian, X. (2024). Optimal sensing of urban road networks with large-scale ride-sourcing vehicles. Arxiv preprint arxiv: 2207.11285.

He, Z., Cao, J., & Liu, X. (2015). High quality participant recruitment in vehicle-based crowdsourcing using predictable mobility. IEEE Conference on Computer Communications (INFOCOM), Kowloon, Hong Kong, 2542-2550.

Han, K., Ji, W., Nie, Y. (Marco), Li, Z., Liu, S., 2024. Exploring the sensing power of mixed vehicle fleets. Transportation Research Part B: Methodological. 190, 103066.

Iwase, Y. (2026). Nash implementation of stable matchings with multi-unit demand and weak priorities. Economics Letters, 264, 112958.

Ji, W., Han, K., & Liu, T. (2023). A survey of urban drive-by sensing: An optimization perspective. Sustainable Cities and Society, 104874.

Jaillet, P. , Qi, J. , & Sim, M. (2016). Routing optimization under uncertainty. Operations Research, 64(1).

Kwon, H., & Shorrer, R. I. (2026). Justified-envy-minimal efficient mechanisms for priority-based matching. Games and Economic Behavior, 157, 71–87.

Khan, J.A., Ghamri-Doudane, Y., & Botvich, D. (2016). Autonomous identification and optimal selection of popular smart vehicles for urban sensing - An information-centric approach. IEEE Transactions on Vehicular Technology, 65(12), 9529-9541.

Liu, Y., Niu, J., & Liu, X. (2016). Comprehensive tempo-spatial data collection in crowd sensing using a heterogeneous sensing vehicle selection method. Personal and Ubiquitous Computing, 20(3), 397-411.

Liu, S., Ge, Q., Han, K., Fukuda., D., & Dantsuji., T. (2025). Mechanism design for coordinating vehicle-based mobile sensing tasks within the ride-hailing platform.Transportaion Research Part C: Emerging Technologies,105151.

Martino, S.D., & Lucio Starace, L.L. (2022). Vehicular crowd-sensing on complex urban road networks: A case study in the city of Porto. Transportation Research Procedia, 62, 350-357.

Masutani, O. (2015). A sensing coverage analysis of a route control method for vehicular crowd sensing. In 2015 IEEE International Conference on Pervasive Computing and Communication Workshops (PerCom Workshops) (pp. 396-401).

Mathur, S., Jin, T., Kasturirangan, N., Chandrasekaran, J., Xue, W., Gruteser, M., & Trappe, W. (2010). Parknet: drive-by sensing of road-side parking statistics. In Proceedings of the 8th international conference on Mobile systems, applications, and services (pp. 123-136).

Ng, M.W., & Lo, H. K. (2016). Robust models for transportation service network design. Transportation Research Part B Methodological, 94(dec.), 378-386.

O'Keeffe, K. P., Anjomshoaa, A., Strogatz, S. H., Santi, P., & Ratti, C. (2019). Quantifying the sensing power of vehicle fleets. Proceedings of the National Academy of Sciences, 116(26), 12752-12757.

Pasqualetti, F., Durham, J. W., & Bullo, F. (2012). Cooperative patrolling via weighted tours: Performance analysis and distributed algorithms. IEEE Transactions on Robotics, 28(5), 1181-1188.

Qi, J. , Sim, M. , Sun, D. , & Yuan, X. (2016). Preferences for travel time under risk and ambiguity: implications in path selection and network equilibrium. Transportation Research Part B Methodological, 94(dec.), 264-284.

Riahi, V., Hakim Newton, M.A., & Sattar, A. (2021). A scatter search algorithm for time-dependent prize-collecting arc routing problems. Computers & Operations Research 134,105392.

Scarf, H. (1957). A min-max solution of an inventory problem. Studies in the Mathematical Theory of Inventory & Production.

Sidiropoulos, S. , Han, K. , Majumdar, A. , & Ochieng, W. Y. (2017). Robust identification of air traffic flow patterns in metroplex terminal areas under demand uncertainty. Transportation Research Part C: Emerging Technologies, 75(FEB.), 212-227.

Song, J., Han, K., & Stettler, M. E. (2021). Deep-MAPS: Machine learning based mobile air pollution sensing. IEEE Internet of Things Journal, 8(9), 7649-7660.

Tonekaboni, N.H., Ramaswamy, L., Mishra, D., Setayeshfar, O., & Omidvar, S. (2020). Spatio-temporal coverage enhancement in drive-by sensing through utility-aware mobile agent selection. In: Song, W., Lee, K., Yan, Z., Zhang, LJ., Chen, H. (eds) Internet of Things - ICIOT 2020. ICIOT 2020. Lecture Notes in Computer Science, vol 12405, pp. 108-124. Springer, Cham: Springer International Publishing.

Viti, F., Rinaldi, M., Corman, F., &Tampére, C.M.J. (2014). Assessing partial observability in network sensor location problems. Transportation Research Part B: Methodological, 70,65-89.

Wu, Y., Wang, Y., Wang, L., Song, G., Gao, J., Yu, L., 2020. Application of a taxi-based mobile atmospheric monitoring system in Cangzhou, China. Transportation Research Part D: Transport and Environment, 86, 102449.

Wang, Y.Y., Li, J.H., Song, D.N., & Zhou, L.(2026). Personnel assignment method for cruise ship production design considering task execution continuity with priority and skill matching constraints. Computers & Industrial Engineering, 212, 111672.

Wang, W., Wu, S., Wang, S., Zhen, L., & Qu, X. (2021). Kaivonen location problems in logistics: Status and perspectives. Transportation research part E: logistics and transportation review, 154:102465.

Xu, S., Chen, X., Pi, X., Joe-Wong, C., Zhang, P., & Noh, H.Y. (2020). iLOCuS: Incentivizing vehicle mobility to optimize sensing distribution in crowd sensing. IEEE Transactions on Mobile Computing, 19, 1831-1847.

Yi, K., Du, R., Liu, L., Chen, Q., & Gao, K. (2017). Fast participant recruitment algorithm for large-scale Vehicle-based Mobile Crowd Sensing. Pervasive and Mobile Computing 38, 188-199.

Yang, B., Han, K., Liu, S., & Li, R. (2025). Joint matching and pricing for taxi drive-by sensing. Transportation Research Part E: Logistics and Transportation Review, 197, 104071.

Yu, H. , Fang, J. , Liu, S. , Ren, Y. , & Lu, J . (2021). A node optimization model based on the spatiotemporal characteristics of the road network for urban traffic mobile crowd sensing. Vehicular Communications, 31, 100383.

Zhao, D., Ma, H. & Liu, L. (2014). Energy-efficient opportunistic coverage for people-centric urban sensing. Wireless Netw, 20, 1461–1476.

Zhang, X., Yang, Z., & Liu, Y., (2018). Vehicle-based bi-objective crowdsourcing. IEEE Transactions on Intelligent Transportation Systems, 19 (10), 3420-3428.

Zhang, Y., Zhang, Z., Lim, A., & Sim, M. (2021). Robust data-driven vehicle routing with time windows. Operations Research, 69(2), 469-485.

Zhu, N., Fu, C., & Ma, S. (2018). Data-driven distributionally robust optimization approach for reliable travel-time-information-gain-oriented traffic sensor location model. Transportation Research Part B: Methodological, 113(JUL.), 91-120.

Zhao, D., Ma, H., Liu, L., & Li, X. (2015). Opportunistic coverage for urban vehicular sensing. Computer Communications, 60, 71-85.